Ultrasonic-Assisted Drilling of Cortical and Cancellous Bone in a Comparative Point of View

Sousan Pourgiv
University of Isfahan
Nima Jamshidi
nima.jamshidi.phd@gmail.com
University of Isfahan
Aminollah Mohammadi
Isfahan University of Technology
Alireza Mosavar
University of Tehran

Research article

Keywords: Bone Drilling, Ultrasonic-Assisted Drilling, Conventional Drilling, SEM Imaging, Histopathology, Finite Element Analysis

Posted Date: April 2nd, 2021

DOI: https://doi.org/10.21203/rs.3.rs-368773/v1

Version of Record: A version of this preprint was published at Heliyon on March 1st, 2024. See the published version at https://doi.org/10.1016/j.heliyon.2024.e26248.

Abstract

Background: A potential method in drilling of bone is ultrasonic-assisted drilling. In addition, during the drilling of bone, which is common in clinical surgeries, excessive heat generation and drilling force may lead to damages in bone tissue, and thus to failure of implants and fixation screws or delay in healing process. The aim of this study was to appraise efficiency of ultrasonic-assisted drilling in comparison to conventional drilling.

Methods: In addition to investigating drilling force and temperature elevation, their effects on arising osteonecrosis and micro-cracks were explored in ultrasonic-assisted and conventional drilling through histopathologic assessment and microscopic imaging. In this regard, three drilling speeds and two drilling feed-rates were considered as drilling variables in the *in-vitro* experiments. Moreover, numerical modeling gave an insight into temperature distribution during drilling process in the both methods and compared three different vibration amplitudes.

Results: Although temperature elevations were lower in the conventional drilling, the ultrasonic-assisted drilling had lesser drilling forces. Furthermore, the latter method had smaller osteonecrosis regions, and did not have micro-cracks in cortical bone and destructions in structure of cancellous bone.

Conclusions: The ultrasonic-assisted drilling, which caused lesser damages to the bone tissue in both cortical and cancellous bone, was more comparatively advantageous.

Introduction

Drilling of the bone is common in orthopaedic surgeries and prosthodontics; however, conventional drilling causes considerable thermal and mechanical damages in drilling site [1]. The thermal damages can lead into ‘thermal osteonecrosis’, which is loss of blood supply for bone cells due to excessive heat and consequent death of the cells (osteocytes). It is believed that the thermal osteonecrosis is because of drilling force, friction, and resulted heat [2]. Presence of empty osteocyte lacunae is a pathological distinction for this phenomenon. On the other hand, the mechanical damages owing to applied force include micro-cracks in the mineralized matrix of bone, which can cause ‘osteocytes apoptosis’ [3]. While some of the micro-cracks may disappear during the remodeling process, some others can damage bone structure [4]. Hence, during the drilling, it is important to control amount of both the generated heat and the applied force for drilling since the outcome of the surgery depends on them strongly. The necrosis and apoptosis of osteocytes affect ‘osseointegration’ and the healing process, and can increase risk of loosening and failure in implants and screws [5].

To control the risk of micro-cracks and thermal osteonecrosis, the aim of this *in-vitro* study was to investigate the efficiency of ultrasonic-assisted drilling (known also as ‘ultrasonic drilling’) in both cortical and cancellous bone, and to compare it to normal conventional drilling. The ultrasonic drilling is a drilling method in which high frequency vibrations (more than 20 KHz) are applied to the longitudinal axis of the drilling bit [6]. For the above-mentioned comparison, the control of osteonecrosis was evaluated with

temperature variations and histopathological assessments. Furthermore, the control of micro-cracks was appraised through determination of mean applied force for drilling and through scanning electron microscope (SEM) assessments. In addition, the experiments were conducted in entire combinations of three different drilling feed-rates and two different drilling speeds. The last but not the least was our *in-silico* study on the temperature distribution during drilling with the both methods through finite element analysis. In addition to casting lights on the experimental results, it gave us the opportunity to investigate the effect of vibration amplitude in ultrasonic drilling.

Materials And Methods

1. **Bone Specimens**

For *in-vitro* drilling, ovine lumbar vertebrae was employed which includes both cortical and cancellous bone. Ovine bone is common in orthopaedic animal-experiments due to its similar properties to human bone [7-10]; however, according to the comparative body of this study, any possible discrepancy in bone properties does not actually hurt deductions [5]. Fresh bones were prepared for drilling according to the literature [11]. It is noteworthy to mention that although body blood flow acts as coolant during drilling *in-vivo*, it is negligible based on literature [12].

2. **Drilling of Bone**

To compare the two drilling methods in the same drilling conditions except considering ultrasonic vibrations for ultrasonic method, we designed and implemented a setup, including an ultrasonic assembly for drilling, a drill bit with 4 mm diameter, a dynamometer (for measuring mean drilling force), and an industrial CNC milling machine (Figure 1). The ultrasonic assembly provided the optional vibration for ultrasonic drilling with frequency of 20 KHz and amplitude of 20 μm. Moreover, three drilling speeds of 500, 1200, and 2000 rpm and two drilling feed-rates of 30 and 60 mm per minute were considered [13-15]. Each vertebral bone was drilled with the both drilling methods and similar drilling parameters. Furthermore, to ensure the precision and validity of results, each experiment was repeated twice more.

3. **Investigation of Temperature Variations**

In order to record temperature variations during drilling, we used type K thermocouple [5, 16]. The distance between drilling site and thermocouple site was 0.5 mm and the depth in which thermocouple was placed in the bone was 10 mm [5]. In addition, the room temperature was 22 °C and the bones warmed up to the same temperature.

4. **Histopathological and SEM Evaluation**

For histopathological study, first, specimens were decalcified in nitric acid solution. After keeping in formalin, one-half of their circular section was prepared for SEM imaging while the second half needed

further processing for histopathological evaluation. Therefore, the latter half of each specimen was kept in alcohol solution for dehydration process. Then, after employing xylene and paraffin wax, specimens were sliced with microtome machine to have longitudinal sections of the holes and surrounding tissues. Finally, hematoxylin and eosin were used for staining. To assess osteonecrosis around each hole, under an optical microscope, the radius of region in which more than 90% of osteocyte lacunas were empty was considered.

The first mentioned half of each specimen was considered for examining the micro-cracks in the bone. Hence, after a dehydration process, a SEM was used to capture images from the surface of each hole with 80x and 200x magnifications.

5. **Finite Element Modeling**

To have a better insight into our experimental results, finite element method was implemented for numerical modeling of the both drilling methods. Finite element analysis is inherently an approximation tool; however, applicable approximations and simplifications can be employed and still have realistic models in which important aspects of the problem are taken into account [17, 18]. Since we knew the chip removal mechanism is identical in 2-dimensional and 3-dimentional models [19], to avoid time-consuming and expensive simulations, we considered 2-dimensional models [19-21]. In the modeling, bone structure was considered as an isotropic elastic-plastic material that was dependent on strain rate, and the Johnson-Cook model was used to define the plastic behavior. The required thermal and mechanical properties of the drill bit (made of 316L stainless steel) and the bone were obtained from the literature [22-24] (Table 1). According to our experimental drilling speeds, a linear speed of 400 mm/s was used. In addition, with a vibration frequency of 20 KHz, three different amplitude of 10, 15, and 20 μm were modeled for ultrasonic drilling. Finally, friction coefficient was 0.3 for surface-to-surface contacts in the models. The aim of these simulations was to study the pattern of temperature distribution in each drilling method, while as we also investigated the influence of vibration amplitude in ultrasonic drilling.

Results

1. **Temperature Variations and Drilling Forces**

Numerical results of the study are presented in Table 2, which shows maximum achieved temperature and mean required force during each experiment. However, for having a better look at differences of the drilling methods in various conditions, Figure 2a and Figure 2b also diagramed the outcomes for temperature and mean force, respectively. According to these figures, while in the conventional drilling, the feed-rate had minimal effect on the temperature rise, its effect in the ultrasonic drilling was dramatic. Furthermore, the drilling force had a direct relationship with the feed-rate and an inverse relationship with the drilling speed.

The experimental outcome of dynamometer in Figure 3 casts a glance at the qualitative differences of instantaneous drilling forces in the two drilling methods. As seen in the figure, with regard to the feed-rate

and the drilling depth, drilling duration was 10 seconds. Moreover, although the force peaked in the both drilling methods during passing the cortical region of the bones (which is more dense and harder than cancellous region as also seen in Table 1) [25], the apex was much higher in the conventional drilling. Another noticeable point was oscillations in the force magnitude during drilling cancellous region due to its spongy structure; however, the changes were higher again in the conventional drilling.

2. **Histopathological and SEM Evaluation**

Figure 4 illustrates an example of our histopathological observations, which shows a region around drilling site that has multiple empty osteocyte lacunae. According to our observations, the osteonecrosis region was greater in the cortical bone in comparison to the cancellous bone, and it was much greater in the specimens of the conventional drilling in comparison to the ultrasonic drilling. The greatest osteonecrosis region was for the conventional drilling with drilling speed of 500 rpm and feed-rate of 60 $mm.min^{-1}$ (Figure 4) that was approximately 1.1 mm in the cortical bone and 0.4 mm in the cancellous bone. With regard to the Figure 2, this specimen had one of the lowest temperature rises, but the highest drilling force. In spite of smaller osteonecrosis regions in other specimens of the conventional drilling, notably in the cortical bone, the amount of osteonecrosis was higher than entire specimens of the ultrasonic drilling were. It is noteworthy that in the conventional drilling, the amount of osteonecrosis roughly did not change in the cancellous bone.

For the ultrasonic drilling, we observed the greatest osteonecrosis region in the specimen for drilling speed of 1200 rpm and feed-rate of 30 $mm.min^{-1}$ that was approximately 0.6 mm in the cortical bone and 0.4 mm in the cancellous bone. With regard to the Figure 2, in contrast to the above-mentioned specimen of the conventional drilling method, this specimen had one of the lowest drilling forces, but the highest temperature rise. However, the difference for osteonecrosis in the cortical region is very considerable. Eventually, the least osteonecrosis, in the both cortical and cancellous bone, was in the specimen of the ultrasonic drilling with drilling speed of 2000 rpm and feed-rate of 60 $mm.min^{-1}$ that was approximately 0.2 mm in the cortical bone and 0.2 mm in the cancellous bone.

The results of SEM imaging were used for investigation of micro-cracks propagation in the bone structure. While with the conventional drilling, there were multiple micro-cracks in the cortical region of the bone and the cancellous region was destroyed (Figure 5a and Figure 5b), with the ultrasonic drilling, there was no micro-cracks in the cortical bone and the spongy structure of cancellous bone remained preserved (Figure 5c and Figure 5d).

3. **Finite Element Analysis**

According to the simulations, in the conventional drilling, the temperature rise occurred only in created chip (Figure 6a), while in the ultrasonic drilling, in addition to the chip, the temperature rise in cutting edge of the bone was also considerable (Figure 6b). This difference in the temperature distribution of the two methods, which was observed in both cortical and cancellous bone models, can explain the difference in

the recorded maximum temperatures around the drilling site in the experiments; in fact, the temperature rise in the cutting edge could affect the recorded temperature more since it remained in the bulk bone.

Moreover, with increasing the vibration amplitude from 10 to 15 and then to 20 μm, the temperature rise as well as the temperature distribution in the cutting edge of the bone also increased (Figure 6c and Figure 6d). On the other hand, we compared the required force in these three conditions and it decreased with increasing the amplitude while they were all lower than the force in the conventional drilling simulation.

4. **Statistical Analyses**

To detect the influence of the drilling methods and parameters (the factors) on the mean drilling force and the temperature (the outcomes), we employed analysis of variance (ANOVA) and studied the significance of each factor and their interaction on the outcomes. According to Table 3, *F*- and *P*-value indicate that effect of all three factors on the force and the temperature was significant (*P*-value ≤ 0.05). Whereas the drilling method was the most effective factor on the both outcomes with the highest contribution, drilling speed had completely different level of effectiveness on them; in spite of having roughly negligible influence on the temperature, it affected the force considerably. Regarding the feed-rate, while it had very high effect on the temperature, its contribution on the force was still noticeable. According to 2-way interactions, only the interaction between the drilling method and speed had significant effect on the force, and evidently, the most effective interaction for the temperature was between the drilling method and the feed-rate.

Discussion

In the literature, in recent years, there was a growing interest on studying the efficiency of ultrasonic drilling in bone [6, 14, 15, 26-31]. However, each study had its own drilling parameters that made their outcomes specific. On the other hand, all of them investigated the application of ultrasonic drilling only in cortical bone. In this study, with considering optimum drilling parameters based on previous findings, we studied both the cortical and cancellous bone. In addition, we not only investigated the drilling force [6, 26, 28] and the temperature rise [14, 15, 27-31], but also assessed their effects: the necrosis and apoptosis of osteocytes through histopathologic evaluation [14, 15] in addition to the micro-cracks propagation and mechanical damages with SEM imaging. Finally, employing finite element modeling gave us an insight into the temperature distribution during each drilling method.

With regard to temperature, many previous studies on ultrasonic drilling in bone only focused on determination of temperature changes [27, 29-31] since its elevation is claimed as a marker for osteonecrosis [2, 32]. However, studies on the comparison of ultrasonic drilling and conventional drilling based on the temperature elevation are not consistent. Alam et al [27] studied ultrasonic drilling with frequency range of 5 to 30 KHz and their results showed lower temperatures for frequencies below 20 KHz in comparison to conventional drilling with the same drilling parameters. Ironically, here, with the frequency of 20 KHz, our results were thoroughly in a starling contrast to this outcome and the contrast

was more significant in the lower feed-rates (Figure 2a). Furthermore, they claimed that vibration amplitude did not affect the temperature rise, which is in opposition to the results of our finite element analysis, again. There is also similar contrary view in some other studies [14, 26, 29]. Despite these contraries, there are also some supports for our results on comparison of temperature elevation in the literature [15, 30, 31]. As our finite element analyses also implied, the temperature distribution differed in the two drilling methods, which can explain the higher temperature elevation in the ultrasonic drilling. Bai et al [31] believe that in this method, the superposed motion intensifies the friction motion at the interface of the drill body and the wall of the bone hole, which leads to intensive heat generation there.

Concerning the mean force, our results on the competence of ultrasonic drilling in comparison to conventional drilling (Figure 2b) was completely in accordance to the previous studies [6, 28]. Shakouri et al [26] also indicated the same outcome for drilling speed of 1000 rpm. It is claimed that ultrasonic drilling causes lower drilling force and torque in comparison to conventional drilling by changing the mechanism of chip formation [6]. However, in the study of Shakouri et al, the temperature rise for ultrasonic drilling with drilling speed of 2000 rpm was negligible and independent of feed-rate that our results disagreed over the both.

Comparing Figure 2a with Figure 2b, to explain the trends, we can state that increasing the feed-rate raises friction and therefore the mean force, which yields into generating more heat. However, as the feed-rate increases, the drilling time falls, resulting in lower transmission of generated heat to the bone and lesser temperature elevation. On the other hand, as the drilling speed goes up, the amount of frictional energy that is generated by drill bit increases; and since most of the drilling energy is converted to heat, increasing the rotational speed raises the temperature of the bone [33].

The attention-grabbing comparative point in the results, notably in the diagrams of Figure 2, is that in the one hand, we found lower temperature elevation for the conventional drilling, and on the other hand, the ultrasonic drilling had better results for drilling force. However, the temperature elevation and the force are not the main interests in application, and their influences on osteonecrosis and mechanical damages are what we should care for. As mentioned above, the former finding about the advantage of the conventional drilling could indicate less osteonecrosis yield in comparison to the ultrasonic drilling, especially since it was considerable for the feed-rate of 30 $mm.min^{-1}$. Nevertheless, according to the later finding on the competitiveness of ultrasonic drilling in the required force, the believe that the osteonecrosis is because of drilling force and friction, and that the mechanical damages owing to applied force can cause osteocytes apoptosis could cast doubts on the superiority of the conventional drilling method. In addition, the cumulative effect of the force magnitude and the temperature rise was not clear. Therefore, our histopathologic observations, as explained in the result section, were interesting, especially since these observations were supported by the outcomes of SEM imaging. Consequently, we can conclude that the ultrasonic drilling was more comparatively advantageous based on the bone damages in both cortical and cancellous bone. The results showed death of osteocytes was not only due to temperature elevation, but also because of the drilling force, and both these parameters should be

considered to assess the bone damages. This is in good agreement with some previous findings in the literature [15, 34].

However, more *in-vivo* studies on clinical success of the ultrasonic drilling are needed, both on animals and on human. Moreover, to have a better conclusion, consideration of further drilling parameters may be helpful.

Conclusion

In this study, appraising the effects of the drilling force and the temperature rise on the necrosis and apoptosis of osteocytes, as well as the micro-cracks propagation and mechanical damages, provided a novel understanding on the efficiency of ultrasonic-assisted drilling in cortical and cancellous bone. Through comparing the ultrasonic-assisted drilling with conventional drilling, although we achieved lesser temperature elevations in the latter method, the former method had lower drilling forces. In conclusion, based on our observations on histopathology of the bone tissue and on SEM imaging of the drilling surface, the ultrasonic-assisted drilling was more comparatively advantageous.

List Of Abbreviations

Not applicable.

Declarations

Ethics approval and consent to participate: Not applicable.

- Consent for publication: Not applicable.

- Availability of data and material: All data generated or analyzed during this study are included in this published article.

- Competing interests: The authors declare that they have no competing interests.

- Funding: There was not funding available for this study.

- Authors' Contributions: Conception or design of the work by Sousan Pourgiv and Nima Jamshidi; acquisition, analysis, and interpretation of data for the work by all authors; drafting the work by Alireza Mosavar; and revising it critically by all authors.

- Acknowledgements: The authors declared no acknowledgements related to this study.

References

1. Draenert FG, Mathys Jr R, Ehrenfeld M, Draenert Y, Draenert K (2007) Histological Examination of Drill Sites in Bovine Rib Bone after Grinding in vitro with Eight Different Devices. *British Journal of Oral Maxillofacial Surgery* 45: 548-552.
2. Karaca F, Aksakal B (2013) Effects of Various Drilling Parameters on Bone during Implantology: An in vitro Experimental Study. *Acta of Bioengineering and Biomechanics* 15: 25-32.
3. Noble B (2003) Bone Microdamage and Cell Apoptosis. *European Cells and Materials* 6: 46-56.
4. Gupta V, Pandey PM, Silberschmidt VV (2017) Rotary Ultrasonic Bone Drilling: Improved Pullout Strength and Reduced Damage. *Medical Engineering and Physics* 41: 1-8.
5. Effatparvar MR, Jamshidi N, Mosavar A (2020) Appraising Efficiency of OpSite as Coolant in Drilling of Bone. *Journal of Orthopaedic Surgery and Research*, 15: 197.
6. Alam K, Mitrofanov A, Silberschmidt VV (2011) Experimental Investigations of Forces and Torque in Conventional and Ultrasonically-Assisted Drilling of Cortical Bone. *Medical Engineering and Physics* 33: 234-239.
7. Wan S, Lei W, Wu Z, Liu D, Gao M, Fu S (2010) Biomechanical and Histological Evaluation of an Expandable Pedicle Screw in Osteoporotic Spine in Sheep. *European Spine Journal* 19: 2122-2129.
8. Yurttutan ME, Kestane R, Keskin A, Dereci O (2016) Biomechanical evaluation of oversized drilling on implant stability-an experimental study in sheep. *Journal of Pakistan Medical Association* 66: 147-150.
9. Lopez CD, Alifarag AM, Torroni A, Tovar N, Diaz-Siso JR, Witek L, Rodriguez ED, Coelho PG (2017) Osseodensification for Enhancement of Spinal Surgical Hardware Fixation. *Journal of the Mechanical Behavior of Biomedical Materials* 69: 275-281.
10. McGovern JA, Griffin M, Hutmacher DW (2018) Animal Models for Bone Tissue Engineering and Modelling Disease. *Disease Models and Mechanisms* 11: dmm033084.
11. Wang W, Shi Y, Yang N, Yuan X (2014) Experimental Analysis of Drilling Process in Cortical Bone. *Medical Engineering and Physics* 36: 261–266.
12. Augustin G, Zigman T, Davila S, Udillijak T, Staroveski T, Brezak D, Babic S (2012) Cortical Bone Drilling and Thermal Osteonecrosis. *Clinical Biomechanics* 27: 313–325.
13. Augustin G, Davila S, Mihoci K, Udiljak T, Vedrina SD, Antabak A (2008) Thermal Osteonecrosis and Bone Drilling Parameters Revisited. *Archives of Orthopaedic and Trauma Surgery* 128: 71-77.
14. Singh G, Jain V, Gupta D, Sharma A (2018) Parametric Effect of Vibrational Drilling on Osteonecrosis and Comparative Histopathology Study with Conventional Drilling of Cortical Bone. *Proceedings of the Institution of Mechanical Engineers, Part H* 232: 975-986.
15. Alam K, Al-Ghaithi A, Piya S, Saleem A (2019) In-vitro Experimental Study of Histopathology of Bone in Vibrational Drilling. *Medical Engineering and Physics* 67: 78-87.
16. Sezek S, Aksakal B, Karaca F (2012) Influence of Drill Parameters on Bone Temperature and Necrosis: A FEM Modelling and in vitro Experiments. *Computational Materials Science* 60: 13–18.

17. Mosavar A, Ziaei A, Kadkhodaei M (2015) The Effect of Thread Design on Stress Distribution in a Dental Threaded Implant under Consideration of Bone Anisotropy and Different Osseointegration Conditions: A Finite Element Analysis. *International Journal of Oral and Maxillofacial Implants* 30: 1317-1326.
18. Mosavar A, Hashemi SR, Nili M, Kadkhodaei M (2017) A Comparative Analysis on Two Types of Oral Implants, Bone-level and Tissue-Level, with Different Cantilever Lengths of Fixed Prosthesis. *Journal of Prosthodontics* 26: 289-295.
19. Alam K, Mitrofanov A, Silberschmidt VV (2010) Thermal Analysis of Orthogonal Cutting of Cortical Bone Using Finite Element Simulations. *International Journal of Experimental and Computational Biomechanics* 1: 236-251.
20. Alam K, Mitrofanov A, Silberschmidt VV (2009) Finite Element Analysis of Forces of Plane Cutting of Cortical Bone. *Computational Materials Science* 46: 738-743.
21. Santiuste C, Rodríguez-Millán M, Giner E, Miguélez H (2014) The Influence of Anisotropy in Numerical Modeling of Orthogonal Cutting of Cortical Bone. *Composite Structures* 116: 423-431.
22. Wagnac E, Arnoux PJ, Garo A, Aubin CE (2012) Finite Element Analysis of the Influence of Loading Rate on a Model of the Full Lumbar Spine under Dynamic Loading Conditions. *Medical and Biological Engineering and Computing* 50: 903-915.
23. El-Rich M, Arnoux PJ, Wagnac E, Brunet C, Aubin CE (2009) Finite Element Investigation of the Loading Rate Effect on the Spinal Load-Sharing Changes under Impact Conditions. *Journal of Biomechanics* 42: 1252-1262.
24. Chen YC, Tu YK, Tsai YJ, Tsai YS, Yen CY, Yang SC, Hsiao CK (2018) Assessment of Thermal Necrosis Risk Regions for Different Bone Qualities as a Function of Drilling Parameters. *Computer Methods and Programs in Biomedicine* 162: 253-261.
25. Li Z, Yang D, Hao W, Wu T, Wu S, Li X (2016) A Novel Technique for Micro-Hole Forming on Skull with the Assistance of Ultrasonic Vibration. *Journal of the Mechanical Behavior of Biomedical Materials* 57: 1-13.
26. Alam K, Khan M, Silberschmidt VV (2013) Analysis of Forces in Conventional and Ultrasonically Assisted Plane Cutting of Cortical Bone. *Proceedings of the Institution of Mechanical Engineers, Part H* 227: 636-642.
27. Alam K, Silberschmidt VV (2014) Analysis of Temperature in Conventional and Ultrasonically-Assisted Drilling of Cortical Bone with Infrared Thermography. *Technology and Health Care* 22: 243-252.
28. Shakouri E, Sadeghi MH, Karafi MR, Maerefat M, Farzin M (2015) An in Vitro Study of Thermal Necrosis in Ultrasonic-Assisted Drilling of Bone. *Proceedings of the Institution of Mechanical Engineers, Part H* 229: 137-149.
29. Zheng Q, Xia L, Zhang X, Zhang C, Hu Y (2018) Reduction Thermal Damage to Cortical Bone Using Ultrasonically-Assisted Drilling. *Technology and Health Care* 26: 843-856.

30. Sun Z, Wang Y, Xu K, Zhou G, Liang C, Qu J (2019) Experimental Investigations of Drilling Temperature of High-Energy Ultrasonically Assisted Bone Drilling. *Medical Engineering and Physics* 65: 1-7.
31. Bai X, Hou S, Li K, Qu Y, Zhang T (2019) Experimental Investigation of the Temperature Elevation in Bone Drilling Using Conventional and Vibration-Assisted Methods. *Medical Engineering and Physics* 69: 1-7.
32. Udiljak T, Ciglar D, Skoric S (2007) Investigation into Bone Drilling and Thermal Bone Necrosis. *Advances in Production Engineering and Management* 2: 103–112.
33. Lee J, Chavez CL, Park J (2018) Parameters Affecting Mechanical and Thermal Responses in Bone Drilling: A Review. *Journal of Biomechanics* 71: 4-21.
34. Karaca F, Aksakal B, Kom M (2011) Influence of Orthopaedic Drilling Parameters on Temperature and Histopathology of Bovine Tibia: An in Vitro Study. *Medical Engineering and Physics* 33: 1221-1227.

Tables

Table 1: Thermal and mechanical characteristics of the drill bit and the bone.

Characteristic	Drill Bit	Cortical Bone	Cancellous Bone
Density ($Kg.m^{-3}$)	7,990	1,830	170
Poisson's Ratio	0.25	0.30	0.25
Modulus of Elasticity (MPa)	193×10^{3}	14×10^{3}	291
Yield Stress (MPa)	290	110	1.92
Ultimate Stress (MPa)	579	155	2.23
Hardening Modulus (MPa)	–	100	20
Hardening Exponent	–	0.1	1.0
Failure Plastic Strain	–	9.68×10^{-3}	14.5×10^{-3}
Strain Rate Coefficient	–	0.272	0.533
Reference Strain Rate	–	1	1
Specific Heat Capacity ($J.Kg^{-1}.°C^{-1}$)	500	1,640	1,477
Thermal Conductivity ($W.m^{-1}.K^{-1}$)	16.2	0.452	0.087

Table 2: The numerical results of the entire experiments.

Drilling Parameter		Maximum Temperature (°C)		Drilling Force (N)	
Feed-Rate ($mm.min^{-1}$)	Drilling Speed (rpm)	Conventional Drilling	Ultrasonic Drilling	Conventional Drilling	Ultrasonic Drilling
30	500	25.8 ± 0.5	36.7 ± 1.4	9.59 ± 0.3	3.65 ± 0.7
30	1200	25.9 ± 1.0	38.9 ± 0.9	6.16 ± 0.6	3.38 ± 0.3
30	2000	28.0 ± 1.5	37.1 ± 1.3	4.91 ± 0.1	2.72 ± 0.2
60	500	25.7 ± 0.9	27.3 ± 0.9	12.23 ± 0.9	5.20 ± 0.4
60	1200	25.0 ± 0.1	29.7 ± 0.5	7.15 ± 1.1	4.36 ± 0.5
60	2000	28.2 ± 0.2	29.3 ± 0.2	6.28 ± 0.3	4.05 ± 0.3

Table 3: The results of statistical analyses (ANOVA) for the entire experiments. In the table the following codes are used; DM for drilling method, FR for feed-rate ($mm.min^{-1}$), and DS for drilling speed (rpm).

Source	Analyses for the Force			Analyses for the Temperature		
	Contribution	F-Value	P-Value	Contribution	F-Value	P-Value
Model	96.62%	82.64	0.000	96.58%	81.57	0.000
Linear	83.38%	160.45	0.000	74.10%	140.80	0.000
DM	50.58%	389.30	0.000	49.41%	375.58	0.000
FR	7.52%	57.92	0.000	22.36%	169.96	0.000
DS	25.28%	97.29	0.000	2.32%	8.83	0.001
2-Way Interactions	13.24%	20.38	0.000	22.48%	34.18	0.000
DM × FR	0.12%	0.94	0.342	19.61%	149.04	0.000
DM × DS	12.38%	47.63	0.000	2.59%	9.83	0.001
FR × DS	0.74%	2.85	0.076	0.29%	1.10	0.347

Figures

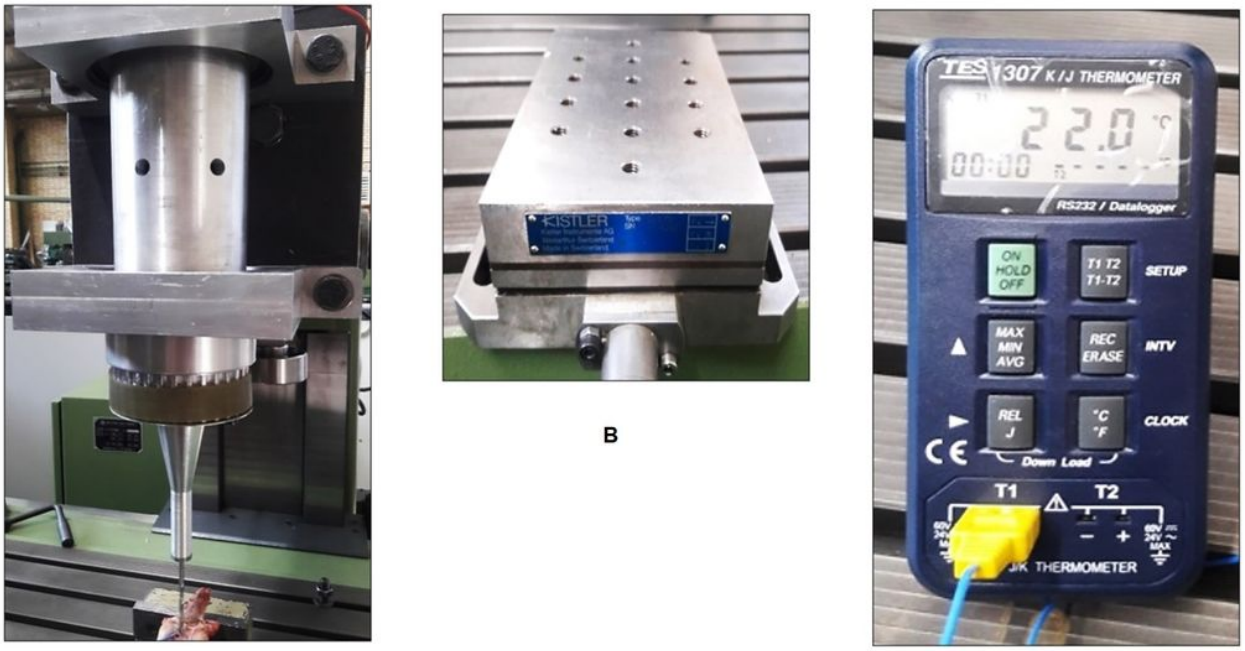

Figure 1

The experimental setup for drilling of bones, and for temperature and force measurements. The employed CNC milling machine had options for regulation of drill speed and feed-rate. Moreover, the maximum bone temperatures during drilling were measured with two thermocouples. a) Ultrasonic assembly for drilling; b) Dynamometer; c) Dual-channel data logger (for recording temperatures).

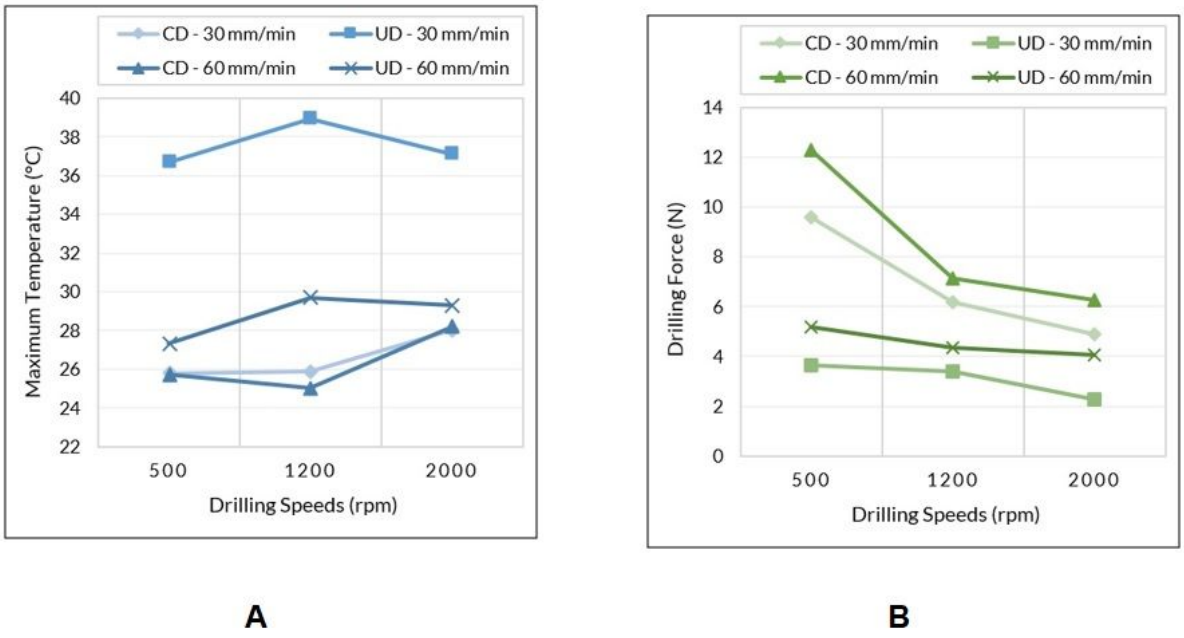

Figure 2

a) Diagram of recorded maximum temperatures in experiments; b) Diagram of mean drilling forces in experiments. In the diagrams, CD represents conventional drilling method and UD denotes ultrasonic drilling method.

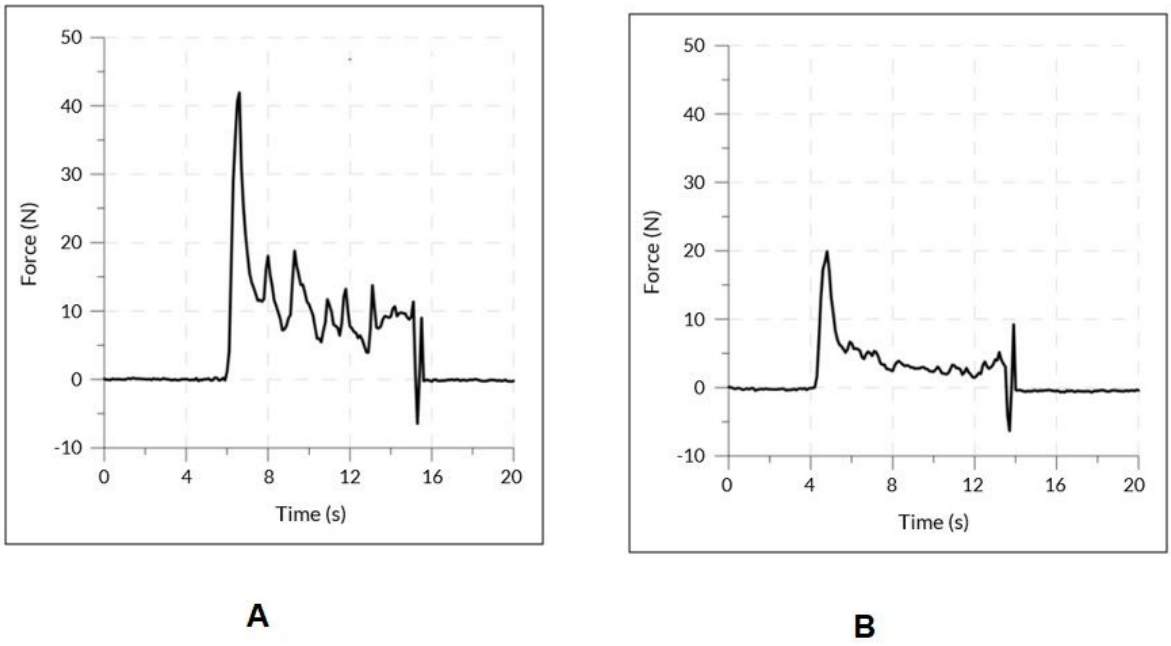

Figure 3

The experimental force-time diagrams (based on dynamometer outcomes) with drilling speed of 500 rpm and feed-rate of 60 mm.min-1 for a) the conventional drilling and b) the ultrasonic drilling.

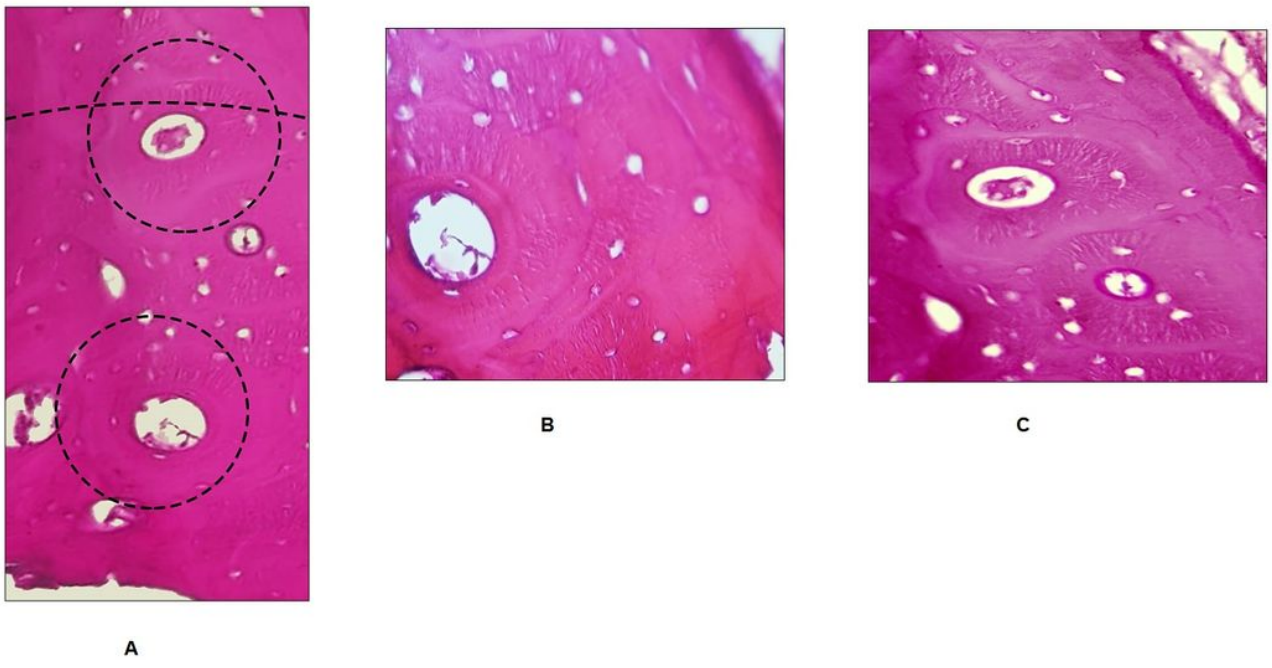

Figure 4

a) Image of bone tissue with 100x magnification around drilling site in the specimen of cortical bone in the conventional drilling with drilling speed of 500 rpm and feed-rate of 60 mm.min-1. The drilling edge is on the inferior side of this image and a crossed line shows the osteonecrosis region. On the superior side of this image, less than 90% of osteocyte lacunae are empty. In addition to osteocyte lacunae, some Haversian canals are observed. b) Image of bone tissue with 400x magnification from the osteonecrosis region with empty lacunae. c) Image of bone tissue with 400x magnification from the region between empty lacunae and undamaged osteocytes.

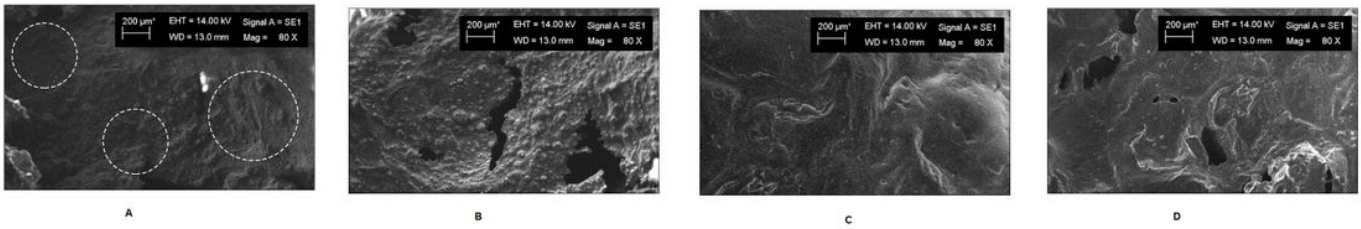

Figure 5

a) SEM image of bone surface around drilling site in the conventional drilling method for the specimens with drilling speed of 500 rpm and feed-rate of 60 mm.min-1 and with 80x magnification, in the cortical bone that micro-cracks can be seen, and b) in its cancellous bone that the spongy structure was ruined. c) SEM image of bone surface around drilling site in the ultrasonic drilling method for the specimens with drilling speed of 1200 rpm and feed-rate of 30 mm.min-1 and with 80x magnification, in the cortical bone, and d) in its cancellous bone that the spongy structure is maintained.

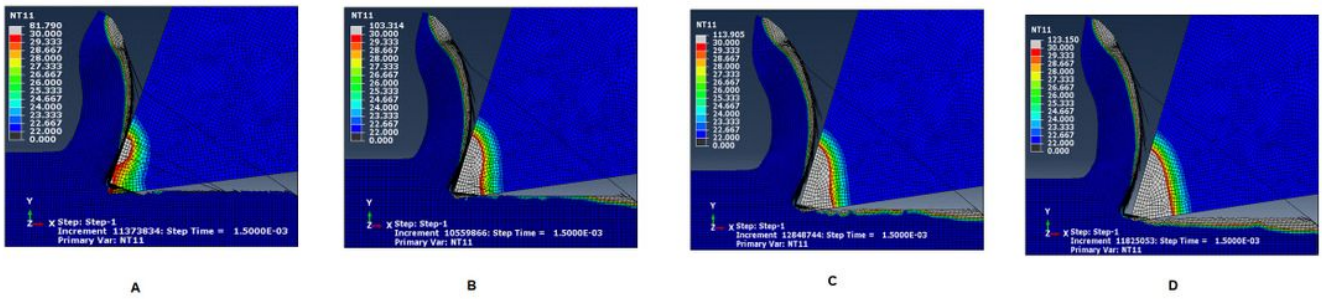

Figure 6

Temperature distribution in the cutting edge and the drilled chip of cortical bone in a) the conventional drilling, and in the ultrasonic drilling with vibration amplitudes of b) 10 μm, c) 15 μm, and d) 20 μm.